

1 **COMPARATIVE LIFE CYCLE ASSESSMENT OF** 2 **HIGH-YIELD SYNTHESIS ROUTES FOR CARBON** 3 **DOTS**

4
5 Sónia Fernandes^a, Joaquim C.G. Esteves da Silva^{a,b}, Luís Pinto da Silva^{a,b*},

6 ^a Chemistry Research Unit (CIQUP), Faculty of Sciences of University of Porto, R. Campo
7 Alegre 697, 4169-007 Porto, Portugal;

8 ^b LACOMEPhi, GreenUPorto, Department of Geosciences, Environmental and Territorial
9 Planning, Faculty of Sciences of University of Porto, R. Campo Alegre 697, 4169-007 Porto,
10 Portugal;

11 * Correspondence: luis.silva@fc.up.pt

12 13 **Abstract**

14 Carbon dots (CDs) are carbon-based nanomaterials with advantageous luminescent properties,
15 making them promising alternatives to other molecular and nanosized fluorophores. However,
16 the development of CDs is impaired by the low synthesis yield of standard fabrication strategies,
17 making high-yield strategies essential. To help future studies to focus on cleaner production
18 strategies, we have employed a Life Cycle Assessment (LCA) to compare and understand the
19 environmental impacts of available routes for the high-yield synthesis of carbon dots. These
20 routes were: (1) production of hydrochar, via hydrothermal treatment of carbon precursors, and
21 its alkaline-peroxide treatment into high-yield carbon dots; (2) thermal treatment of carbon
22 precursors mixed in a eutectic mixture of salts. Results show that the first synthesis route is
23 associated with the lowest environmental impacts. This is attributed to the absence of the mixture
24 of salts in the first synthesis route, which offsets its higher electricity consumption. Sensitivity
25 analysis showed that the most critical parameter in the different synthetic strategies is the identity
26 of the carbon precursor, with electricity being also relevant for the first synthesis route.
27 Nevertheless, the use of some carbon precursors (as citric acid) with higher associated
28 environmental impacts may be justified by their beneficial role in increasing the luminescent
29 performance of carbon dots. Thus, the first synthesis route is indicated to be the most
30 environmental benign and should be used as a basis in future studies aimed to the cleaner and
31 high-yield production of carbon dots.

32
33 **Keywords:** Life Cycle Assessment; Carbon Dots; Engineered Nanomaterials; High-Yield
34 Synthesis; Green Chemistry; Fluorescence

35 **1. Introduction**

36 Carbon dots (CDs) are fluorescent carbon-based nanomaterials, with either an amorphous
37 or nanocrystalline core, and a surface on which can be found different functional groups
38 (Esteves da Silva and Gonçalves, 2011; Wang et al., 2017a; Zhou et al., 2017). CDs have
39 several remarkable properties, such as strong luminescence (Xiong et al., 2018; Wang et al.,
40 2013), water solubility (Lim et al., 2015), good physical-chemical and photochemical stability
41 (Lim et al., 2015; Kozák et al., 2013; Sendão et al., 2018), low toxicity (Wang et al., 2013)
42 and biocompatibility (Baker and Baker, 2010; Sun et al., 2006; Vale et al., 2020). Given this,
43 it is not surprising that CDs have been increasingly used in several applications, such as in
44 sensing (Crista et al., 2019; Liu et al., 2021; Mello et al., 2019; Qiu et al., 2020; Simões et al.,
45 2020), bioimaging (Kang et al., 2015; Bogireddy et al., 2020; Ding et al., 2020), photocatalysis
46 (Li et al., 2021), in light-emitting devices (Wang et al., 2019; Wang et al., 2017b; Qiao et al.,
47 2020), drug delivery (Hettiarachchi et al., 2019), solar cells (Yan et al., 2016) and in
48 photodynamic therapy (He et al., 2018; Knoblauch and Geddes, 2020).

49 Another attractive characteristic of CDs is that they can be produced by using a wide variety
50 of precursors without sophisticated equipment, via simple solvothermal, thermal or
51 microwave-assisted treatment of organic molecules, which are used as a carbon source (Crista
52 et al., 2020a; Zhou et al., 2018a; Crista et al., 2020b; Zhou et al., 2018b; Tripathi et al., 2016;
53 Yang et al., 2016). While CDs can be prepared from a great number of organic molecules,
54 most of them can still be expensive, and their use and/or synthesis can pose significant
55 challenges to the environment and human health (Zhang et al., 2019). Given this, biomass has
56 been increasingly used as a precursor for the synthesis of CDs due to its abundance, low cost,
57 renewability, and sustainability (Algarra et al., 2019; Crista et al., 2020a; Xie et al., 2019; Zhao
58 et al., 2015). However, it should be noted that there is not a consensus about biomass
59 sustainability, namely due to greenhouse gas (GHG) emissions from bioenergy and biobased
60 materials (van der Hilst et al., 2018).

61 Despite this, one problem that plagues the development of CDs is that their synthesis yields
62 are usually very low (below ~10%) (Christé et al., 2020; Tan et al., 2016; Yang et al., 2012),
63 which hinders their large-scale production and future industrial applications. This low yield is
64 explained by current synthetic strategies generating large amounts of solid carbon material as
65 a major by-product, with the actual amount of CDs in suspension being quite low (Zhang et
66 al., 2018). Thus, as this solid carbon material can be produced by traditional CDs' synthesis
67 in large-scale (as it is the major product), if a strategy could be found to convert it into CDs,
68 the low synthesis yield problem of these nanomaterials could be solved.

69 Indeed, different authors are already focusing on this topic. Namely, Li et al. (2017) were
70 recently able to generate different CDs in high yield (25.8-66.7%) from different carbon
71 precursors in a two-step process. First, a carbon source and a eutectic mixture of molten salts

72 were mixed to promote polymerization and then by a carbonization process to generate CDs. In
73 the next step, the mixture was dissolved in water, and by a dialysis process to remove salts as well
74 as products with low molecular weight (Li et al., 2017). In a similar study, Jing et al. (2019) also
75 produced CDs in high yield by first subjecting an aqueous solution of biomass to hydrothermal
76 treatment (at 200 °C for 6h), resulting in low yield CDs in suspension (less than 10%) and solid
77 hydrothermal carbon (also described as hydrochar). The hydrochar was then converted into CDs
78 by alkaline-peroxide treatment, by dispersion in NaOH/H₂O₂ solution for 8h at room temperature.
79 This resulted in the production of CDs with a high yield (~20-40%).

80 These studies are very important for the development of new CDs, as they show a way for the
81 large-scale production of nanomaterials. Despite their innovative potential, there can be some
82 doubt regarding which type of strategy should be favored in terms of efficiency and sustainability,
83 as there is limited information regarding the potential environmental impacts generated by these
84 synthetic routes. Such information is essential for determining a suitable strategy for the synthesis
85 of nanomaterials, given that the production steps of engineered nanomaterials have been identified
86 as of environmental concern (Pourzahedi and Eckelman, 2015). Namely, previous studies have
87 determined that the reagents and energy required for the synthesis of engineered nanomaterials
88 can contribute significantly to the environmental impacts generated during their life cycle
89 (Eckelman et al., 2008; Bafana et al., 2018). Given this, it is essential that proposals for large-
90 scale synthesis of a given type of nanomaterials should be first evaluated for their environmental
91 impacts and sustainability, to ensure that attempts to devise improved high-yield routes already
92 take into consideration the best alternatives for cleaner production.

93 Herein, our goal is to assess the environmental impacts associated with the high-yield synthesis
94 of CDs, by analyzing the synthetic strategies proposed by both Li et al. (2017) and Jing et al.
95 (2019). To this end, a life-cycle assessment (LCA) approach will be employed. The aim of LCA
96 is to quantify the environmental impacts of a given system during its life cycle (Ramos et al.,
97 2018a; Ramos et al., 2018b; Hischer and Walser, 2012), making it the most appropriate tool to
98 achieve the goals of the present study. In fact, LCA has already been used with success to evaluate
99 the environmental impacts associated with different types of engineered nanomaterials, such as
100 silver nanoparticles (Bafana et al., 2018; Temizel-Sekeryan and Hicks, 2020), graphene oxide
101 (Deng et al., 2017), copper nanoparticles (Pu et al., 2016), carbon nanotubes (Upadhyayula et al.,
102 2012; Celik et al., 2017; Teah et al., 2020; Temizel-Sekeryan et al., 2021), nanocellulose
103 (Piccinno et al., 2018), TiO₂ nanoparticles (Fernandes et al., 2020), and even CDs (Sendão et al.,
104 2020; Christé et al., 2020). However, a new study about the current state of art in LCA of
105 engineered nanomaterials identifies a scarcity of specific characterization factors regarding the
106 potential impacts related to toxicity, as well as a gap of knowledge about nanomaterial releases
107 into the environment during different life cycle stages, such as their quantities and risks (Salieri
108 et al., 2018).

109 With this study, we expect to identify the high-yield synthesis route with more
 110 sustainability potential, as well as to understand what the most critical parameters are relative
 111 to generated environmental impacts. Given this, we expect to provide a basis for future studies
 112 to provide a cleaner strategy for the high-yield production of CDs.

113

114 2. Methods

115 The experimental section of this study is divided into six sub-sections: Scope and system
 116 boundaries (2.1), Synthesis Routes (2.2), Life Cycle Inventory Data (2.3), Environmental
 117 Impact Assessment (2.4), Sensitivity analysis (2.5), and Scale-Up (2.6), as described below.

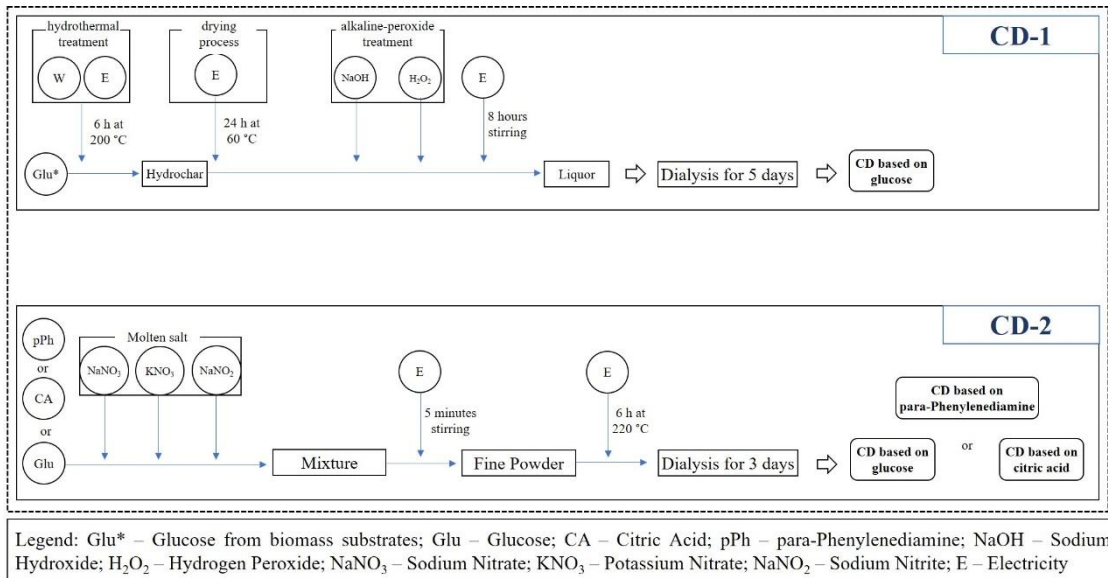
118

119 2.1. Scope and system boundaries

120 The present study is a cradle-to-gate LCA that aims to quantify and compare the potential
 121 environmental impacts, as well as to evaluate the differences between these two types of CDs
 122 syntheses. This study is focused on the laboratory-scale manufacturing stage of target
 123 nanoparticles and considers the direct emissions from CDs production and indirect impacts
 124 associated with upstream resource extraction and energy generation.

125 This work uses two different synthesis routes for the high-yield production of CDs (Li et al.,
 126 2017; Jing et al., 2019), which are described in detail below (Fig. 1).

127



128

129 **Fig. 1.** Diagram for Carbon Dots syntheses.

130

131 The synthesis yield and fluorescence quantum yield of the syntheses under study can be
 132 consulted in Table 1. Synthesis yield is the amount of nanoparticles formed from the used
 133 precursors (in weight, %), while the fluorescence quantum yield is the ratio of photons
 134 absorbed to photons emitted through fluorescence.

135

136 **Table 1.** Properties of both syntheses under study (Li et al., 2017; Jing et al., 2019).

	Synthesis Yield (wt.%)	Quantum Yield (%)
Synthesis 1		
CD based on glucose	40.1	22.67
Synthesis 2		
CD based on glucose	45.5	8.0
CD based on citric acid	39.6	20.8
CD based on <i>para</i> -phenylenediamine	25.8	5.3

137

138 The environmental impacts were analyzed and compared in a first stage by using a weight-
139 based functional unit of 1 kilogram (kg), that is, it was considered 1 kg of produced CDs.

140 Considering a weight-based functional unit is needed to allow compare an equivalent quantity
141 of nanomaterial (Feijoo et al., 2017; Hischer and Walser, 2012). Later, these impacts were
142 normalized by the fluorescence quantum yield (QY) of the CDs under study. This is needed
143 because weight-based functional units do not consider functional benefits for which the
144 nanomaterials were engineered. Thus, a weight-based functional unit analysis of potential impacts
145 might not account that a more resource-intensive synthesis may be justified later in the use stage.
146 Therefore, the QY was chosen as the normalization factor to consider the fluorescent QY of each
147 CD, since this is a relevant property in most of the several CDs applications. Thus, we have
148 defined a functional unit (FU) related to the highest QY of the studied CDs (CD-1, Glucose, Table
149 1). Subsequently, we compared reference flows that relate to the FU for each CD under study,
150 according to the expression $\frac{QY_{REF}}{QY}$ (Li et al., 2017; Jing et al., 2019) (Table 2).

151

152 **Table 2.** Functional unit based on Quantum Yield (QY) for each Carbon Dot under study.

Carbon Dot	Quantum Yield (%)	Reference Flow
CD-1 Glucose	22.67	1.00
CD-2 Glucose	8.00	2.83
CD-2 Acid Citric	20.80	1.09
CD-2 <i>para</i> -phenylenediamine	5.30	4.28

153

154 **2.2. Synthesis Routes**

155 For this study, it was compared two different syntheses for the high-yield production of CDs
156 (Li et al., 2017; Jing et al., 2019), with the used materials and electricity being reported in Table
157 S1. The synthesis yields for each route are presented in Table 1.

158 For the first synthesis route, according to Jing et al. (2019) (from now identified as
159 synthesis 1), glucose was hydrothermally treated for 6 hours at 200 °C, followed by
160 centrifugation to separate the suspension and the obtained hydrochar. The latter was
161 subsequently dried at 60 °C for 24 hours in an oven. The final synthesis step consists of an 8
162 hours alkaline-peroxide treatment of the hydrochar, at room temperature. Namely, the dried
163 hydrochar was dispersed into diluted NaOH solution, with the subsequent addition of H₂O₂.
164 The mixture was left to stirring for 8 hours at room temperature. Pure CDs were obtained after
165 a 5-days dialysis process, which was employed to remove salts and other molecular impurities
166 (Jing et al., 2019).

167 In the second synthesis (from now identified as synthesis 2 (Li et al., 2017)), different
168 materials (glucose, acid citric, or *para*-phenylenediamine) were used as precursors in a eutectic
169 mixture of NaNO₃/KNO₃/NaNO₂ (7:53:40 mass ratio) with a melting point of 140 °C. The
170 synthesis route was initiated by mixing (1:10 mass ration) and ground (for 5 minutes) the
171 carbon precursor and the molten salt, forming a fine powder. The next step was heating the
172 powder at 220 °C for 6 hours, followed by dispersion in water and dialysis for 3 days to remove
173 salts and molecular impurities (Li et al., 2017).

174 CDs obtained by the synthesis 1 procedure are named CD-1, while CDs produced
175 by synthesis 2 are termed CD-2.

176

177 **2.3. Life Cycle Inventory Data**

178 The assessment of the environmental impacts associated with the syntheses of CDs was
179 based on inventory data from laboratory-scale synthesis procedures found in the Ecoinvent®
180 3.5 database. The foreground system of the synthesis procedure consists of chemicals used as
181 raw materials and electricity used for the fabrication process (heating plate, oven). The
182 different processes and chemicals included in this study were modeled with the following data
183 present in the Ecoinvent® 3.5 database (GLO standing for global, and RER for regional market
184 for Europe) as described in Table S2.

185 The amount of chemicals and electricity used are described in Table S1. The dataset used
186 for electricity describes the available electricity data on the medium voltage level in Europe
187 for the year 2014, as described in the Ecoinvent® 3.5 database. As referred above, the
188 electricity considered combined the electricity required for using the heating plate and oven.
189 Given that the authors of the studies under evaluation did not identify the used equipment's,
190 we were forced to use instead standard plates and ovens. By using the same equipment's, we
191 are also ensuring that differences between synthesis routes are not due to equipment-specific
192 issues. Thus, it was considered that the heating and stirring plate used was a Normax Nx1200
193 Analogical magnetic stirrer with heating, which has a power consumption of 500 W. The

194 considered oven was DRY- Line® Prime from VWR, with 12 A and a power supply in AC (single
195 phase) of 230 V which can achieve with a maximum power factor (1) a power consumption
196 maximum of 2760 W.

197

198 **2.4. Environmental Impact Assessment**

199 The present LCA study is based on a cradle-to-gate approach, from the production of precursor
200 materials to the fabrication of CDs. Environmental impacts were modeled using the ReCiPe 2016
201 V1.03 endpoint method, Hierarchist version (Huijbregts et al., 2017), which evaluates three
202 categories of potential impacts (Human Health, Ecosystems and Resources). The Hierarchist
203 perspective is a scientific consensus model to deal with uncertainties and assumptions based on
204 the most common policy principles with regards to the time frame and plausibility of impact
205 mechanisms. In Human Health (HH) subsection were assessed Global Warming – Human Health
206 (GW–HH), Stratospheric ozone depletion (SO), Ionization Radiation (IR), Ozone formation –
207 Human Health (OF), Fine Particulate Matter formation (FPM), Human Carcinogenic toxicity
208 (HC), Human Non-Carcinogenic toxicity (HNC) and Water Consumption – Human Health (WC–
209 HH). Ecosystems (E) potential impacts evaluated were Global Warming – Terrestrial Ecosystems
210 (GW–TE), Global Warming – Freshwater Ecosystems (GW–FE), Ozone Formation – Terrestrial
211 Ecosystems (OF–TE), Terrestrial acidification (TA), Freshwater Eutrophication (FE), Marine
212 Eutrophication (ME), Terrestrial EcoToxicity (TET), Freshwater EcoToxicity (FET), Marine
213 EcoToxicity (MET), Land Use (LU), Water Consumption – Terrestrial Ecosystem (WC–TE) and
214 Water Consumption – Aquatic Ecosystems (WC–AE). Resources (R) subsection assessed were
215 Mineral Resource scarcity (MR) and Fossil Resource scarcity (FR). More information about
216 environmental impact subcategories can be found in Table S3. The LCA study was performed
217 using SimaPro 9.0.0.48 software.

218

219 **2.5. Sensitivity analysis**

220 A sensitivity analysis was performed by considering “What-if” scenarios (Pianosi et al., 2016).
221 These consist of varying the amount and/or identity of the type of materials employed, as well as
222 the amount of required electricity. More specifically, a sensitivity analysis was performed with
223 different scenarios for synthesis 1 and 2, by varying ($\pm 30\%$) the used amounts of either electricity
224 or the carbon precursor. A hypothetical scenario was considered by replacing the carbon precursor
225 (glucose) of synthesis 1 with either citric acid or *para*-phenylenediamine (types of precursors
226 employed on synthesis 2), considering the same synthesis yield. This was made to evaluate if the
227 variation of the carbon precursors has a relevant impact on the overall environmental
228 sustainability of the synthesis 1, but it should be noted that in “real-life” this sort of substitution
229 would invariably lead to a different synthesis yield. Beyond this, it was also considered a final

230 scenario related to electricity production from different countries/regions (Brazil, Europe,
 231 Japan, and US), to determine how the location of electricity production affects the data and
 232 environmental sustainability of the synthesis routes. This is relevant once each country has a
 233 characteristic energy matrix that could influence the potential environmental impacts of CDs
 234 syntheses.

235

236 **2.6. Scale-Up**

237 This LCA also aims to help elucidate some uncertainties regarding the large-scale
 238 production of these CDs. Thus, we have also modeled the scaling up from laboratory scale to
 239 industrial scale. To this end, it was extrapolated the laboratory scale results from the
 240 framework developed by Piccinno et al. (2016), by considering a batch reactor with a volume
 241 between 100 L and 1000 L to achieve processing quantities of 100 kg and 1000 kg. The amount
 242 of materials used (glucose, citric acid, *para*-phenylenediamine, NaOH, H₂O₂, H₂O, NaNO₃,
 243 KNO₃ and NaNO₂) were scaled linearly up to the processing quantity. By its turn, the
 244 electricity was scaled based on the framework of Piccinno et al. (2016) that determines the
 245 energy required for the heating and stirring.

246 The heating energy required for the syntheses is determined by Equation (1), in C_p is the
 247 specific heat capacity of the main solvent (J/K/kg), m_{mix} the mass of the reaction mixture (kg),
 248 T_r the reaction temperature (K), T_0 the starting temperature (K), T_{out} the temperature outside
 249 the reactor (K), A surface area of the reactor (m²), k_a the thermal conductivity of the insulation
 250 material (W/m+K), s the thickness of the insulation (m), t the time of the reaction (h) and η_{heat}
 251 the efficiency of the heating device in % (Piccinno et al., 2016).

252

$$253 \quad Q_{react} = \frac{Q_{heat} + Q_{Loss}}{\eta_{heat}} = \frac{C_p \times m_{mix} \times (T_r - T_0) + A \times \frac{k_a}{s} \times (T_r - T_{out}) \times t}{\eta_{heat}} \quad (1)$$

254

255 It was considered that the C_p parameter for the solvent in synthesis 1 refers to water, while
 256 in synthesis 2 refers to the molten salt (NaNO₃/KNO₃/NaNO₂). In this sense, the specific heat
 257 capacity of the molten salt was estimated according to the C_p of the solid phase of each
 258 compound, as obtained in the study of Kawakami et al. (2004) and the ratio of each compound
 259 in the synthesis. In this sense, C_p of the molten salt was determined by the expression
 260 $\frac{C_{p(NaNO_3)} \times 7g}{100g} + \frac{C_{p(KNO_3)} \times 53g}{100g} + \frac{C_{p(NaNO_2)} \times 40g}{100g}$. The remaining parameters were obtained
 261 considering the synthesis in question (CD-1 or CD-2), as well as the values suggested by
 262 Piccinno et al. (2016).

263 On the other hand, the stirring energy was determined by Equation (2), in which N_p is the
 264 type of the impeller (dimensionless number), ρ_{mix} the density of the reaction mixture (kg/m³),

265 N the rotational velocity of stirring (1/s), d the diameter of the impeller (m), t the reaction time
266 (h) and η_{stir} the efficiency of the agitator in % (Piccinno et al., 2016).

267

$$268 \quad E_{stir} = \frac{N_p \times \rho_{mix} \times N^3 \times d^5 \times t}{\eta_{stir}} \quad (2)$$

269

270 It is noteworthy that, for the heating energy, the reaction time (CD-1 and CD-2: 6 hours) and
271 reaction temperature (CD-1: 200 °C and CD-2: 220 °C) remain the same as in the laboratory scale,
272 as well as the duration of the reaction (CD-1: 128 hours and CD-2: 72 hours) for the stirring
273 energy. The parameters of heating energy and stirring energy for the determination of the
274 electricity in the industrial scale for both syntheses can be found in Table S4.

275 It is worth mentioning that, in addition to heating and stirring energy, synthesis 1 considers
276 the energy required for drying hydrochar. However, it was not possible to model this energy with
277 the framework developed by Piccinno et al. (2016), because of the unknown hydrochar
278 characteristics.

279

280 **3. Results and Discussion**

281 This section is divided into four subsections, synthesis comparison by weight (3.1), synthesis
282 comparison by QY (3.2), sensitivity analysis (3.3), and scale-up (3.4).

283

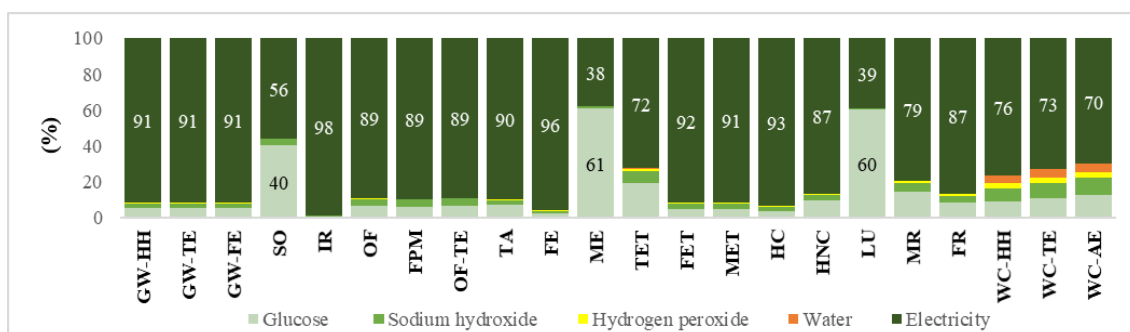
284 **3.1. Synthesis comparison by weight**

285 In a first approach, it was performed a comparison of potential environmental impacts between
286 the syntheses under study by considering a weight-based functional unit of 1 kg of CDs. The
287 results obtained for synthesis 1 are shown in Fig. 2, while the results obtained for synthesis 2 are
288 found in Fig. 3. For this study, our intention was not to make quantitative appreciations of the
289 environmental impacts of each material input, but to compare the contributions to the different
290 impact categories of the input involved in each synthesis and with each other.

291 It was possible to understand that the major contributor for synthesis 1 is, in almost all the
292 environmental impact subcategories, the electricity (with contributions between 56 to 96%).

293 However, the subcategories of Marine Eutrophication (ME) and Land Use (LU) are the
294 exceptions, in which the carbon precursor (glucose) constitutes the highest contribution to
295 environmental impacts in those categories (60-61%). As for hydrogen peroxide and water, their
296 relative contributions appear to be quite negligible.

297



298
299
300
301

Fig. 2. Relative environmental impacts of synthesis 1 (CD-1 based on glucose). Abbreviations are explained in Section 2.4. This graphic was obtained applying ReCiPe endpoint method.

302
303
304
305
306
307
308
309

On the other hand, for the three routes considered for synthesis 2 (each one corresponding to a different carbon precursor), there is not only one major contributor (Fig. 3). For the synthesis routes with either glucose or citric acid (Figs. 3.A and 3.B), sodium nitrite (NaNO_2) appears to predominate in many of these categories. For CD-2 based on glucose, the exceptions are: Stratospheric Ozone depletion (SO) and MR with potassium nitrate (KNO_3) as the highest contributor; IR, Freshwater Eutrophication (FE), Freshwater EcoToxicity (FET), Marine EcoToxicity (MET) and Human Carcinogenic toxicity (HC) with a predominance of electricity; ME and LU have a predominance of glucose.

310
311
312

For CD-2 based on citric acid, the exceptions are: the subcategories GW-HH, GW-TE, GW-FE, SO, and MR with a prevalence of KNO_3 ; IR, FE, and HC show a predominance of electricity; LU and WC-AE show a predominance of citric acid.

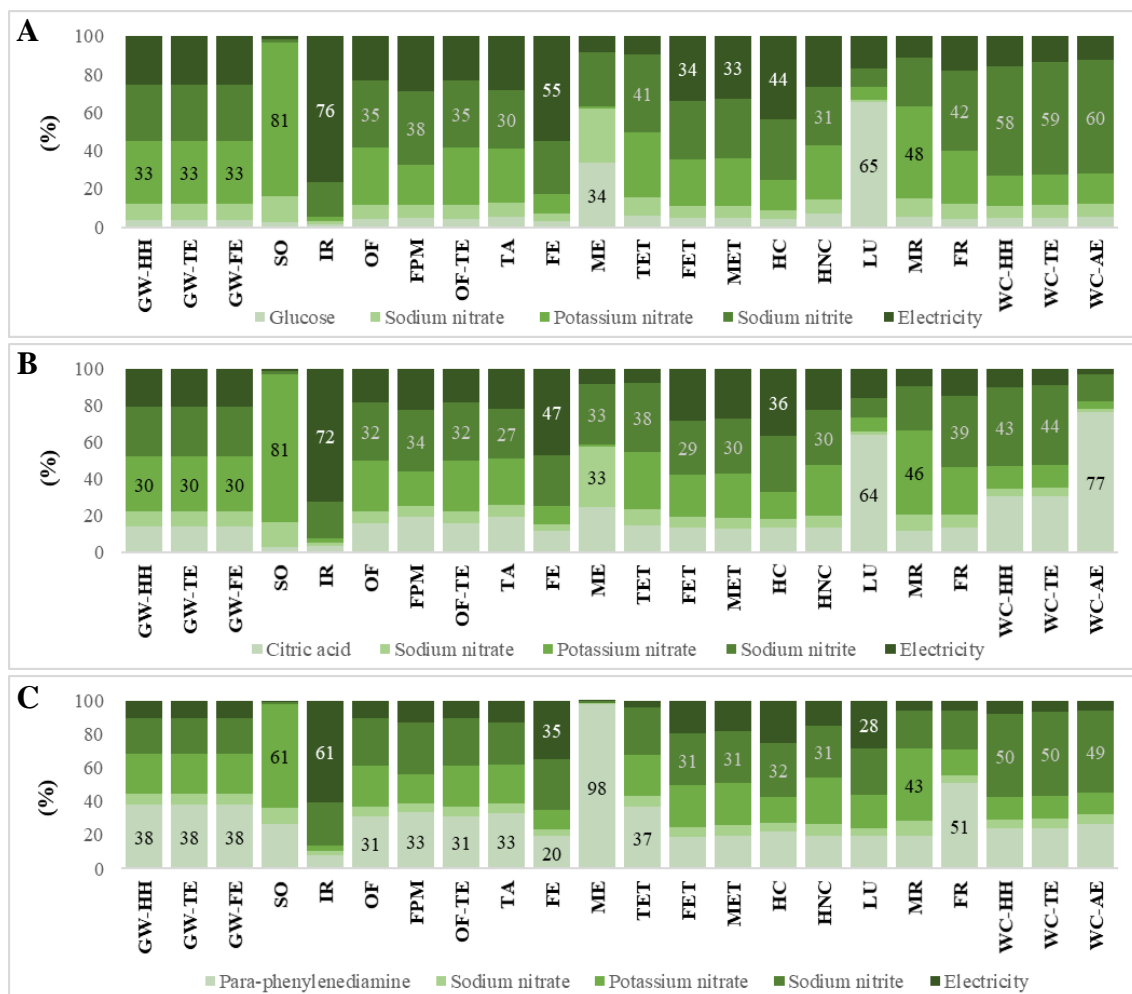
313
314
315
316
317
318

Finally, for CD-2 based on *para*-phenylenediamine (Fig. 3.C), the situation is somewhat different as the contributions of the carbon precursor to associated environmental impacts dominate in many categories (thus, replacing NaNO_2). Nevertheless, the categories SO and MR have KNO_3 as the major contributor, while electricity is the highest contributor to IR, FE, and LU. Finally, NaNO_2 is still the highest contributor in the categories of FET, MET, HC, HNC, WC-HH, WC-TE, and WC-AE.

319
320
321
322
323
324
325
326
327
328

In conclusion, and for synthesis routes (1 and 2), the results indicate that the environmental impacts of both hydrothermal and thermal procedures are caused mainly by the electricity and the carbon precursor (irrespective of its identity), with water being a negligible contributor. The inclusion of salts, such as NaNO_2 and KNO_3 , should lead to higher associated environmental impacts, given their significant contribution in several categories. Interestingly, previous LCA studies of low-yield syntheses of CDs did reveal that electricity is a major contributor for hydrothermal synthesis routes, which is a process that typically requires longer reaction times (of several hours) (Sendão et al., 2020). However, when the synthesis route is microwave-assisted (which generally takes minutes), electricity provides only small to negligible contributions (Sendão et al., 2020). It is worth mentioning that, despite the latter

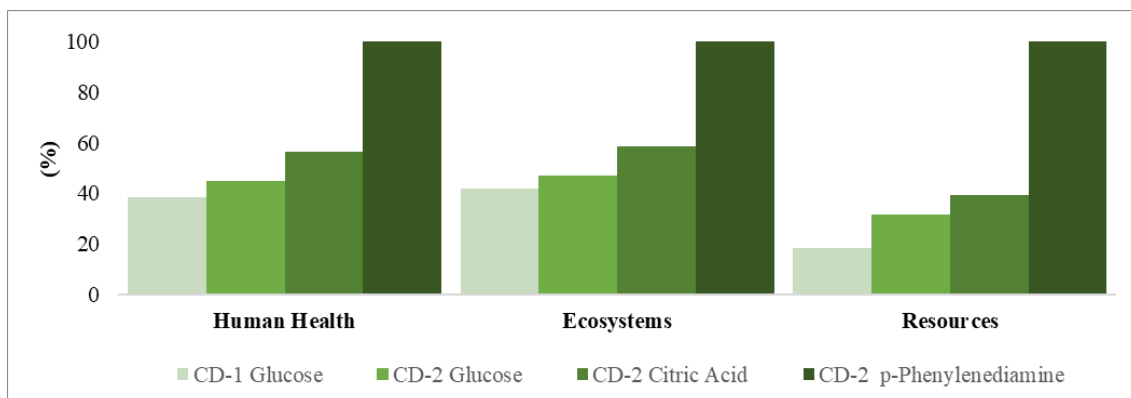
329 processes potentially being more environmentally sustainable due to low electricity consumption
 330 (Sendão et al. 2020), studies show that changing the strategy route (from hydrothermal to
 331 microwave), even with the same precursors, can result in significant alterations in synthesis yield,
 332 quantum yield and other properties (Crista et al., 2020b). Thus, one should be careful before
 333 stating that microwave strategies are indeed more sustainable, as other synthesis strategies could
 334 offset some associated environmental impacts by producing CDs with improved/different
 335 properties.
 336



337
 338 **Fig. 3.** Relative environmental impacts of synthesis 2 of CD based on glucose (A), CD based on citric acid
 339 (B), and CD based on *para*-phenylenediamine (C). The abbreviations are explained in section 2.4. This
 340 graphic was obtained applying ReCiPe endpoint method.
 341

342 To facilitate the comparison between the four studied synthetic routes (one for synthesis 1,
 343 and 3 for synthesis 2), they are compared in the same Figure (Fig. 4), with all environmental
 344 impact subcategories being divided into three main categories: human health, ecosystems, and
 345 resources. The first conclusion is that synthesis 1 is associated with lower environmental impacts
 346 than the routes included under synthesis 2. It should be noted that the amount of carbon precursor

347 is similar in all syntheses, and the electricity used in synthesis 1 is more than the double used
 348 in synthesis 2 (Table S1). Thus, one of the reasons for the higher environmental impacts of the
 349 three routes of synthesis 2, especially for the one with glucose as the carbon precursor (the
 350 same as in synthesis 1), is attributed to the inclusion of the eutectic mixture of salts (as NaNO₂
 351 and KNO₃). This is evident in the SO category where KNO₃ is responsible for 81% of the
 352 impacts, and in water consumption categories in which NaNO₂ is responsible for circa 60% of
 353 impacts.
 354

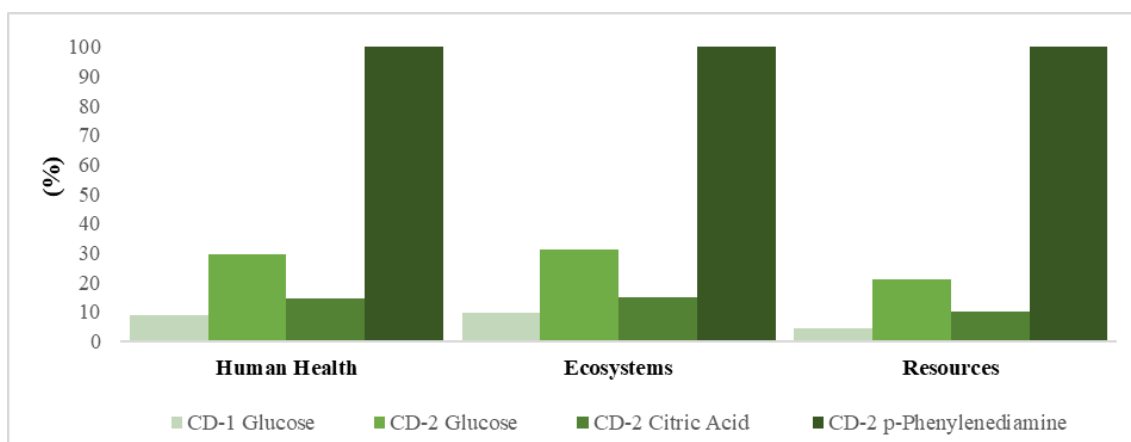


355
 356 **Fig. 4.** Relative environmental impacts of both syntheses (CD-1 and CD-2), considering a comparison by
 357 weight. This graphic was obtained applying ReCiPe endpoint method.

358
 359 Interestingly, the environmental impacts associated with synthesis 2 progressively increase
 360 when the carbon precursor changes from glucose to citric acid and then to *para*-
 361 phenylenediamine. This increase in environmental impacts with different carbon precursors is
 362 higher than the difference caused by the addition of the salts (which can be assessed by
 363 comparing CD-1 and CD-2 from glucose). Thus, we can conclude that the carbon precursor is
 364 a significant contributor to the overall environmental impacts associated with these syntheses,
 365 with citric acid and especially *para*-phenylenediamine being responsible for more
 366 environmental damages than glucose.

367 368 **3.2. Synthesis comparison by QY**

369 It was also evaluated the environmental profiles of each CDs by rescaling their
 370 environmental impacts according to their fluorescence QY (Table 2). The relative
 371 environmental impacts of each synthesis route, according to the QY-based functional unit, are
 372 present in Fig. 5.
 373



374
 375 **Fig. 5.** Relative environmental impacts of both syntheses (CD-1 and CD-2), considering a comparison by
 376 QY. This graphic was obtained applying ReCiPe endpoint method.

377

378 There is a limited qualitative variation that resulted from the re-scaling, as synthesis 1 is still
 379 the one with lower environmental impacts. Also, the route with higher environmental impacts is
 380 still synthesis 2 with the use of *para*-phenylenediamine as a carbon precursor. Nevertheless, one
 381 qualitative difference among the studied synthesis 2 options, is that now the use of citric acid as
 382 the carbon precursor leads to lower environmental impacts than the use of glucose. This is
 383 justified by the fact that the use of citric acid led to CDs with higher QY than the ones with
 384 glucose. In fact, previous LCA studies on CDs indicated that while nitrogen-doping strategies
 385 (typically used to increase the QY of CDs) lead to higher environmental impacts, these are offset
 386 by gains in the QY of the CDs (Sendão et al., 2020). The results here obtained indicate that the
 387 same can also be said for the identity of the carbon precursor.

388 Finally, the results showed that re-scaling did lead to a significant quantitative difference.
 389 Namely, the environmental impacts associated with synthesis 2 with the use of *para*-
 390 phenylenediamine are now even greater than before. This can be explained by *para*-
 391 phenylenediamine, besides being the carbon precursor responsible for higher environmental
 392 impacts, is also the compound that led to lower QY.

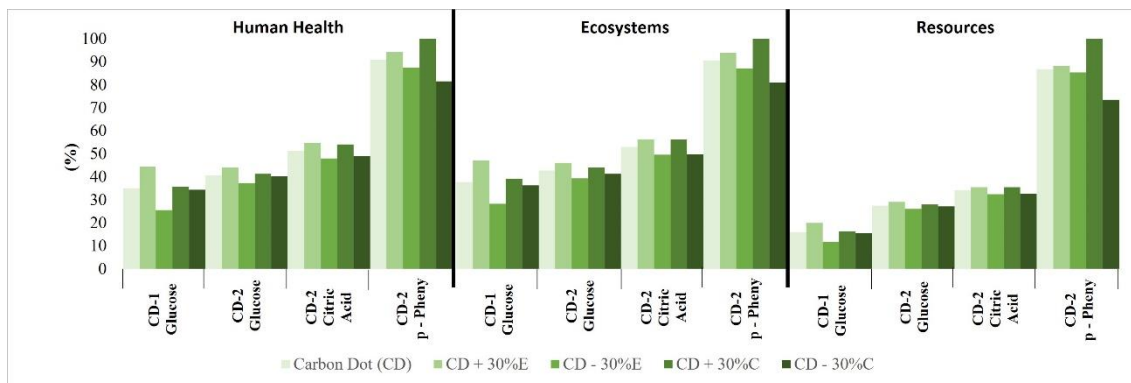
393

394 **3.3. Sensitivity analysis**

395 **3.3.1. Electricity and Carbon Precursor Variation ($\pm 30\%$)**

396 Sensitivity analysis was performed for syntheses 1 and 2. The scenarios consisted of (Fig. 6):
 397 (1) changing the amount ($\pm 30\%$) of electricity used; (2) varying the amount of used carbon
 398 precursor ($\pm 30\%$).

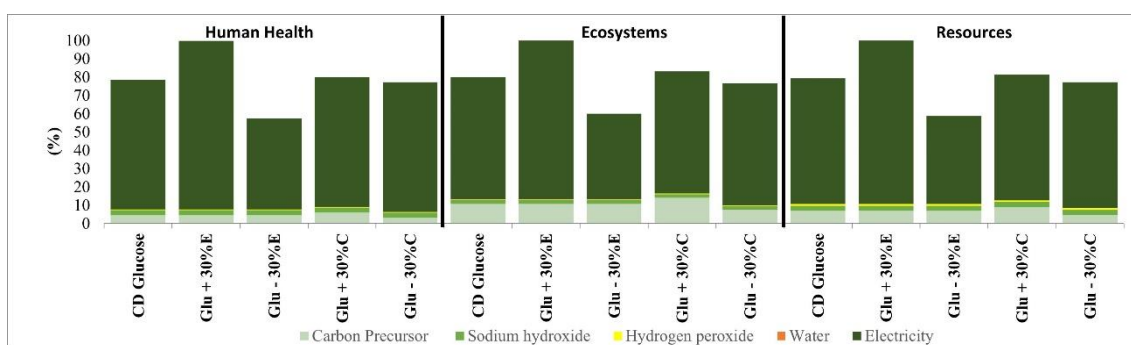
399



400
 401
 402
 403
 404
 405
 406
 407
 408
 409
 410
 411
 412
 413
 414
 415
 416
 417

Fig. 6. Relative environmental impacts for sensitivity analysis of both syntheses (CD-1 and CD-2), considering the variation of electricity or carbon precursor. p-Pheny refers to *para*-phenylenediamine, E refers to Electricity and C refers to Carbon precursor. This graphic was obtained applying ReCiPe endpoint method.

Comparing all syntheses, sensitivity analysis shows that lower environmental impacts (for nearly all categories) are obtained for CD-1 with minus 30% of used electricity. However, when increasing the amount of used electricity, the environmental impacts of CD-1 are now higher than all scenarios for CD-2 with glucose, for Human Health and Ecosystems categories. This indicates the importance that electricity has for the overall environmental impacts associated with CD-1. On the contrary, varying the carbon precursor had a limited impact on the environmental impacts of synthesis 1. More specifically (Fig. S1), for synthesis 1, varying electricity ($\pm 30\%$) represents a variation of 20% in Ecosystems and 21% in Human Health and Resources Categories. On the other hand, considering the carbon precursor for synthesis 1 (Fig. 7), in Human Health the impacts vary 1%, in Ecosystems the variation is 3%, and in Resources vary 2%.



418
 419
 420
 421
 422
 423
 424

Fig. 7. Relative environmental impacts for sensitivity analysis of synthesis 1 (CD-1 based on glucose). Glu refers to Glucose, E refers to Electricity and C refers to Carbon precursor. This graphic was obtained applying ReCiPe endpoint method.

As seen in Fig. 6, varying the amount of either electricity or the carbon precursor has a limited effect on the overall environmental impacts associated with synthesis 2. In fact, the

425 main differences between the three routes of synthesis 2 are still explained by the identity of the
426 used carbon precursor.

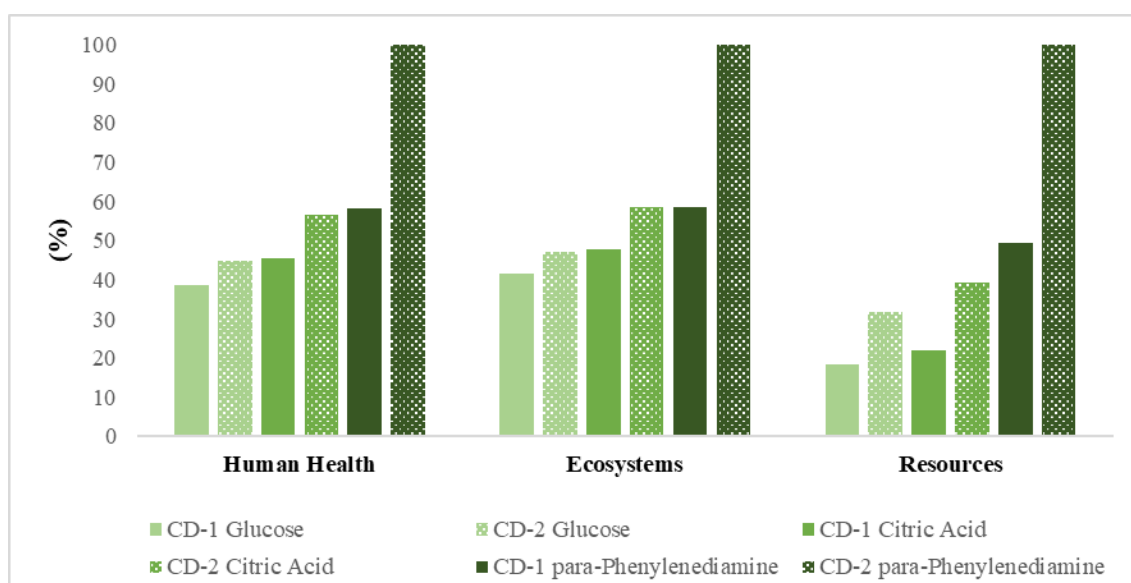
427 For synthesis 2 (Fig. S1), the sensitivity analysis of environmental impacts (decomposed by
428 all inputs) revealed some interesting aspects, since there is an alteration of the highest contributor
429 in some categories. Namely, while for reference CD-2 based on glucose, the highest contributor
430 for all categories is NaNO_2 , the increase of 30% of electricity results in electricity being now the
431 main contributor for Human Health and Ecosystems. For CD-2 based on citric acid, the increase
432 of 30% electricity also results in electricity becoming the highest contributor for the Ecosystem
433 category. Finally, while reference CD-2 based on *para*-phenylenediamine has the carbon
434 precursor as the main contributor in almost all the categories, the decrease of 30% carbon
435 precursor results in NaNO_2 being the highest contributor for the category of Human Health.

436

437 3.3.2. Carbon Precursor variation in synthesis 1

438 It was also performed a sensitivity analysis on synthesis 1 that consists in replacing the carbon
439 precursor (glucose) with either citric acid or *para*-phenylenediamine (Fig. 8).

440



441

442 **Fig. 8.** Relative environmental impacts for sensitivity analysis of both syntheses, with the variation of
443 carbon precursor in synthesis 1. To effects of comparison, all three routes of synthesis 2 are included. This
444 graphic was obtained applying ReCiPe endpoint method.

445

446 This analysis shows that reference CD-1 (glucose as the carbon precursor) remains the most
447 sustainable synthesis, having the lowest impacts on Human Health, Ecosystems, and Resources.
448 Changing the identity of the carbon precursor has obvious effects as the environmental impacts
449 of synthesis 1 increase in a relevant manner by replacing glucose with either citric acid or *para*-
450 phenylenediamine. Moreover, the trend observed before is maintained as increasing

451 environmental impacts are obtained in the following order of carbon precursors: glucose <
452 citric acid < *para*-phenylenediamine. Finally, it should be noted that the environmental
453 impacts of synthesis 1 are always lower than the synthesis 2 route with the same carbon
454 precursor.

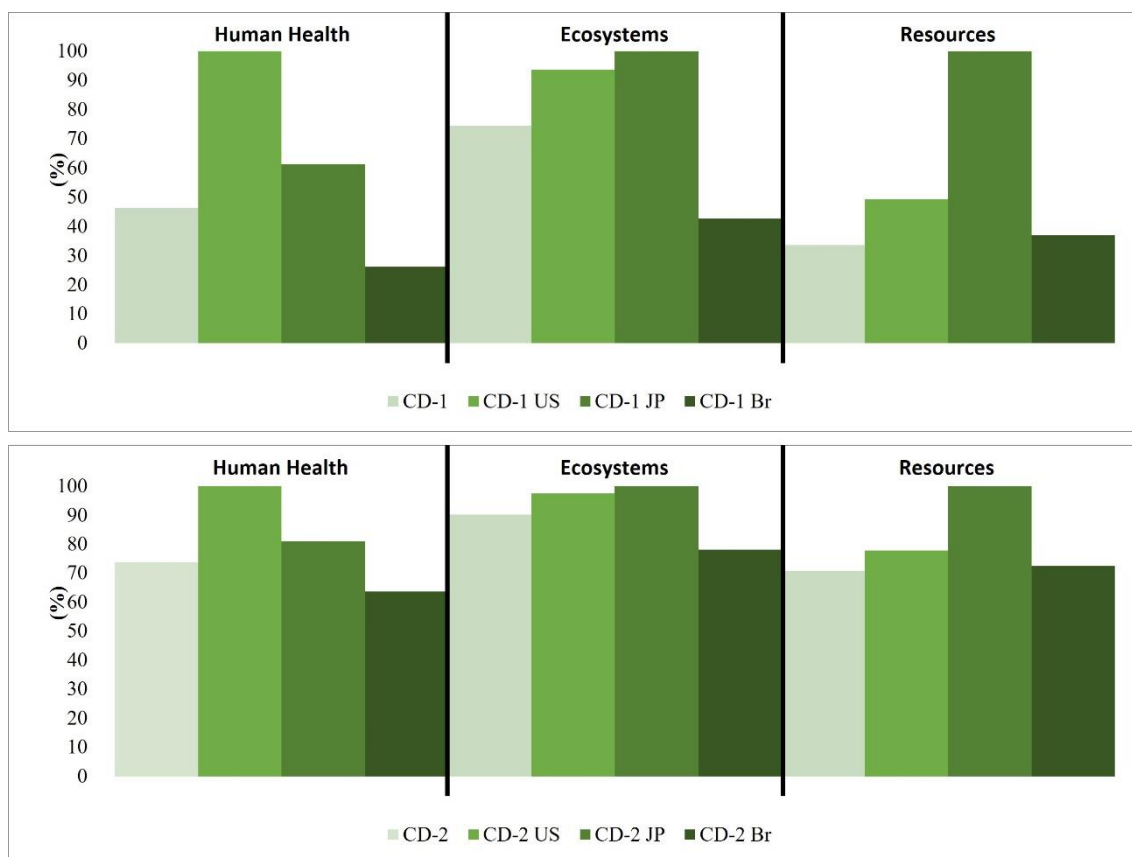
455

456 **3.3.3. Electricity production from different countries**

457 Given that electricity was found to be the main contributor to associated environmental
458 impacts, the final scenario of the sensitivity analysis consisted of varying the region/country
459 in which electricity is generated. That is, a sensitivity analysis (Fig, 9) was performed for the
460 most sustainable CDs of both syntheses (CDs based on glucose), considering other locations
461 for electricity than Europe: United States (US), Japan, and Brazil.

462 The rationale for this type of analysis comes from the fact that different regions/countries
463 possess different energy matrices, with different ratios of high impact/low impact energy
464 sources. In the US, the energy matrix is basically based on coal and natural gas, while in Japan
465 its main energy source is coal (Vinsentin et al, 2019). In Europe, energy production is also
466 reliant on coal, but many countries also have relevant sources of renewable energy (Vinsentin
467 et al, 2019). In fact, an analysis of energy production of all countries in the European
468 Community (carried out by the Ecoinvent database), found the impacts in European scenarios
469 to be smaller than impacts for scenarios for the US and Japan (Vinsentin et al, 2019). Finally,
470 the energy matrix of Brazil is basically composed of clean and renewable energy sources, such
471 as hydroelectric dams (Vinsentin et al, 2019).

472



473
 474 **Fig. 9.** Relative environmental impacts for sensitivity analysis of CD-1 and CD-2 based on glucose with
 475 electricity production from different countries. US refers to the United States, JP to Japan, and Br to Brazil.
 476 This graphic was obtained applying ReCiPe endpoint method.

477
 478 By analyzing the environmental impacts resulting from changing the origin of electricity
 479 production (Fig. 9), it is possible to see that using electricity produced in both the US and Japan
 480 leads to higher environmental impacts than using electricity produced in Europe or Brazil. More
 481 specifically, electricity generated in the US leads to significantly higher impacts in the human
 482 health category, while Japan leads to higher impacts in both the ecosystems (in this case
 483 comparable with electricity produced in the US) and resources categories. Interestingly,
 484 electricity produced in Brazil leads to lower impacts in the human health and ecosystems
 485 categories than electricity produced in Europe, while leading to similar impacts in the resources
 486 category.

487 Our analysis also revealed that CD-1 is more sensitive to variations in the country/region of
 488 origin of used electricity than CD-2. This is not unexpected as electricity is undoubtedly the main
 489 contributor to environmental impacts for CD-1 (71.0-95.5%), while being less relevant for CD-2
 490 (14.9-46.8%) (Table S5).

491 In conclusion, the country/region where the electricity is generated is a sensitive parameter for
 492 the sustainability of these synthesis strategies, particularly for CD-1, with scenarios where

493 electricity is obtained from a matrix of clean/renewable sources leads to significant
494 environmental gains.

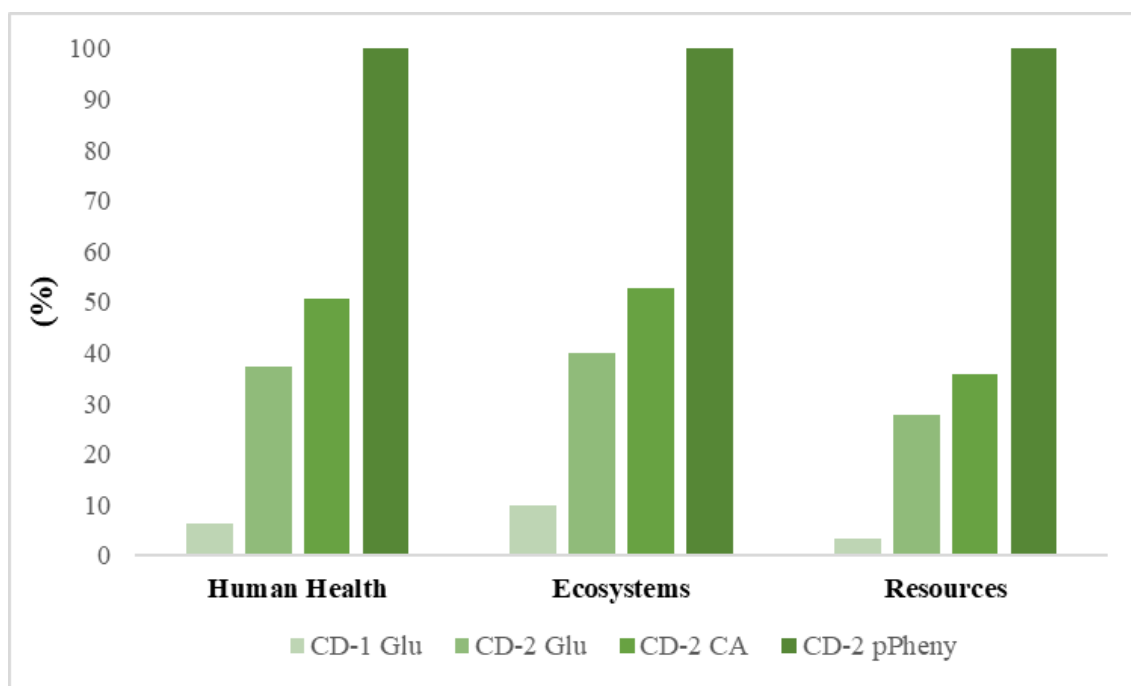
495

496 **3.4. Scale-Up to Industrial Scale**

497 As explained in section 2.6, results at the industrial scale for both synthesis routes (1 and
498 2) were extrapolated from the results obtained at laboratory-scale by considering the
499 framework of Piccinno et al. (2016). Table S6 shows the inventory of raw materials to 100 kg
500 and 1000 kg of each CD under study.

501 This analysis shows (Fig. 10) that, even at an industrial scale, synthesis 1 is still the most
502 sustainable route by a significant percentual margin for all syntheses. In addition, as it is
503 possible to understand by Figure S2, there are no significant differences (<0.1%) between the
504 processing quantity of 100 kg (Fig. S2) and 1000 kg.

505



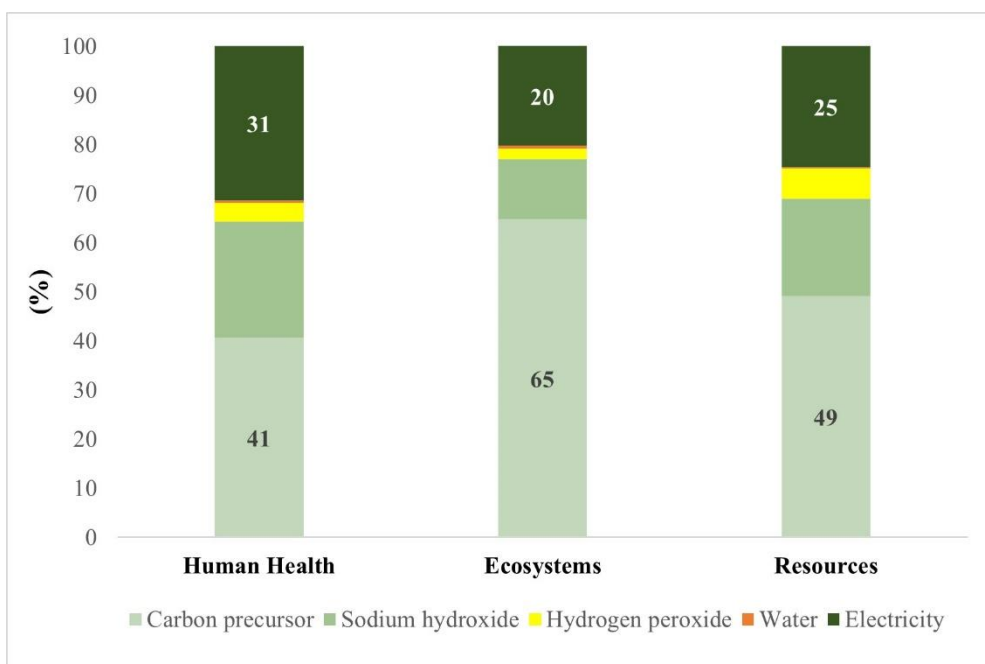
506

507 **Fig. 10.** Relative environmental impacts for scale-up of both syntheses, considering industrial-scale (1000
508 kg). Glu refers to glucose, CA to citric acid, and pPheny to *para*-phenylenediamine. This graphic was
509 obtained applying ReCiPe endpoint method.

510

511 Considering the contribution of each raw material in synthesis 1 (Table S7), the scale-up
512 to 1000 kg reveals that electricity (main contributor at laboratory-scale) constitutes the second
513 main contributor to potential environmental impacts in all categories (HH, E, and R) and that
514 now the carbon precursor occupies the position of the main contributor (Fig. 11).

515



516

517 **Fig. 11.** Relative environmental impacts for scale-up (1000 kg) synthesis 1 in CD based on Glucose. This
 518 graphic was obtained applying ReCiPe endpoint method.

519

520 In synthesis 2, the scale-up of CD based on glucose (Fig. S3) indicates that the main
 521 contributor is still NaNO_2 . Nevertheless, the magnitude of its contributions is higher at an
 522 industrial scale than at a laboratory-scale (Table S8). It is interesting to note that with scale-up,
 523 the contribution of electricity to HH, E, and R decreased from 18-28% to 1-2% (Table S8). The
 524 scale-up of CD-2 based on citric acid (Fig. S4) also reveals that sodium nitrite is still the main
 525 contributor (Table S9), while the contribution from electricity decreased in a similar magnitude
 526 as indicated above (Table S9). Finally, for CD-2 based on *para*-phenylenediamine, the scale-up
 527 to industrial scale (Fig. S5) reveals that carbon precursor is still the main contributor (Table S10),
 528 followed by NaNO_2 .

529 In conclusion, scale-up modeling efforts indicate that the relevance of electricity decreases
 530 significantly for all routes at an industrial scale, becoming even somewhat negligible for synthesis
 531 2. The impacts associated with the use of carbon precursor (for all synthesis routes) and eutectic
 532 mixture of salts (for synthesis 2) are further highlighted.

533 Our approach is aligned with the principles of green chemistry, as its searches for strategies to
 534 prevent waste production during synthetic procedures. Our work focuses on providing researchers
 535 with insight toward the development of a more sustainable high-yield synthesis of CDs, in which
 536 waste generation is reduced. It should be noted that the typical low-yield synthesis of CDs is
 537 associated with the production of ~90% waste. Also, by identifying hotspots of potential impacts
 538 toward the environment and human health, we are helping to devise safer synthetic strategies.

539

540 **4. Conclusions**

541 This work provides the first LCA-based environmental evaluation for high-yield synthesis
542 routes of carbon dots (CDs). Its goal was to understand the environmental performance of two
543 available routes for the large-scale production of CDs, and to provide some considerations that
544 could improve the sustainability of fabricating these engineered nanomaterials of interest.

545 The studied synthesis routes consist of: (1) hydrothermal treatment of carbon precursors to
546 obtain hydrochar material, which is subsequently subjected to alkaline-peroxide treatment to
547 generate CDs with high-yield; (2) thermal treatment of carbon precursors (in powder form)
548 mixed in a eutectic mixture of salts, which generated CDs with high-yield.

549 Analysis of the performance of the syntheses, by considering a weight-based functional
550 unit of 1 kg of produced CDs, showed that synthesis route 1 is associated with the lowest
551 environmental impacts, when comparing with the different options regarding synthesis 2
552 (associated with the possible use of different carbon precursors). In synthesis 1, electricity is
553 the input with the highest environmental impacts in nearly all studied impact categories. The
554 lower relative environmental impacts of synthesis 1 (relative to synthesis 2) were attributed to
555 the absence of the eutectic mixture of salts, used in synthesis 2, which had relevant
556 contributions to several categories of impact.

557 Analysis of synthesis 2, in which different carbon precursors (glucose, citric acid, and *para*-
558 phenylenediamine) were studied, revealed that the identity of the carbon precursor is a key
559 parameter to determine the sustainability of the synthesis route. More specifically, we have
560 found that higher environmental impacts are associated with different carbon precursors in the
561 following trend: glucose < citric acid < *para*-phenylenediamine.

562 A performance-based functional unit (based on the fluorescence quantum yield of the
563 studied CDs) was also used, to understand if functional gains could offset some environmental
564 impacts. Its use still identified synthesis 1 as the fabrication route with the lowest
565 environmental impacts, showing that the formation of hydrochar and its treatment into forming
566 CDs, without the use of other inputs (as a eutectic mixture of salts), can offset its relatively
567 high electricity consumption.

568 A sensitivity analysis was also performed to assess how the environmental impacts of these
569 synthesis routes were affected by variations of the amounts used of carbon precursors and
570 electricity, as well as by replacing the identity of the carbon precursor. Varying the amount of
571 carbon precursor has a not very significant effect on the environmental impacts of the studied
572 synthesis routes. The same can be said for electricity, but just for synthesis 2. However,
573 varying the identity of the carbon precursors led to significant changes in associated
574 environmental impacts for both routes, further showing that this is the most sensitive parameter
575 for the synthesis of CDs, irrespective of the employed synthetic strategy. Scale-up studies

576 indicated that the relevance of electricity decreases significantly for all routes, while the impacts
577 of the carbon precursor are highlighted.

578 In conclusion, synthesis routes based on hydrochar formation and treatment should be favored
579 over strategies focused simply on the thermal treatment of carbon precursors (especially if
580 including extra inputs, such as mixtures of salts). Furthermore, the identity of the carbon
581 precursors is shown to be a critical point in terms of environmental impacts for all studied
582 synthetic strategies. Nevertheless, the environmental impacts resulting from the use of a given
583 carbon precursor can be offset if they lead to better performance in terms of fluorescence quantum
584 yield. Thus, the identity and properties of chosen carbon precursors should become the focus of
585 future studies aiming to a cleaner production of CDs.

586

587 **Acknowledgment**

588 This work was made in the framework of projects UIDB/00081/2020 (CIQUP),
589 UIDB/05748/2020 (GreenUPorto), and PTDC/QUI-QFI/2870/2020. Luís Pinto da Silva
590 acknowledges funding from “Fundação para a Ciência e Tecnologia” (FCT, Portugal) under the
591 Scientific Employment Stimulus (CEECIND/01425/2017). The Laboratory of Computational
592 Modelling of Environmental Pollutants-Human Interactions (LACOMEPhi) is acknowledged.

593

594 **Supplementary Data**

595 Inventory of used materials and electricity, as well as data inventory from Ecoinvent® 3.5
596 database. Parameters of heating and stirring energy for the determination of electricity in the
597 industrial scale for both synthesis routes. Relative environmental impacts to the sensitivity
598 analysis of both syntheses (variation of $\pm 30\%$ electricity, carbon precursor, and country/region of
599 where electricity is generated). Scale-up inventory of raw materials for each CD under study.
600 Relative environmental impacts for the subcategories of Human Health, Ecosystems and
601 Resources for syntheses 1 and 2, relative to scale-up studies.

602

603 **References**

604 Algarra, M., Orfãos, L., Alves, C., Moreno-Tost, R., Pino-González, M., Jiménez-Jiménez, J.,
605 Rodríguez-Castellón, E., Eliche-Quesada, D., Castro, E., Luque, R., 2019. Sustainable Production
606 of Carbon Nanoparticles from Olive Pit Biomass: Understanding Proton Transfer in the Excited
607 State on Carbon Dots. *ACS Sustainable Chem. Eng.*, 7, 12, 10493–10500.
608 <https://doi.org/10.1021/acssuschemeng.9b00969>.

609 Bafana, A., Kumar, S.V., Temizel-Sekeryan, S., Dahoumane, S.A., Haselbach, L., Jeffryes,
610 C.S., 2018. Evaluating microwave-synthesized silver nanoparticles from silver nitrate with life

611 cycle assessment techniques. *Sci. Total Environ.*, *636*, 936-943.
612 <https://doi.org/10.1016/j.scitotenv.2018.04.345>.

613 Baker, S.N., Baker, G.A., 2010. Luminescent carbon nanodots: Emergent nanolights.
614 *Angew. Chem. Int. Ed. Engl.*, *49*, 6726-6744. <https://doi.org/10.1002/anie.200906623>.

615 Bogireddy, N.K., Lara, J., Fragoso, L.R., Agarwal, V., 2020. One-step hydrothermal
616 preparation of highly stable N-doped oxidized carbon dots for toxic organic pollutants sensing
617 and bioimaging. *Chem. Eng. J.*, *401*, 126097. <https://doi.org/10.1016/j.cej.2020.126097>.

618 Celik, I., Mason, B.E., Phillips, A.B., Heben, M.J., Apul, D., 2017. Environmental Impacts
619 from Photovoltaic Solar Cells Made with Single Walled Carbon Nanotubes. *Environ. Sci.*
620 *Technol.*, *51*, 8, 4722–4732. <https://doi.org/10.1021/acs.est.6b06272>.

621 Christé, S., Esteves da Silva, J.C.G., Pinto da Silva, L., 2020. Evaluation of the
622 Environmental Impact and Efficiency of N-Doping Strategies in the Synthesis of Carbon Dots.
623 *Materials* *2020*, *13*(3), 504. <https://doi.org/10.3390/ma13030504>.

624 Crista, D.M.A., Mello, G.P.C., Shevchuk, O., Sendão, R.M.S., Simões, E.F.C., Leitão,
625 J.M.M., Pinto da Silva, L., Esteves da Silva, J.C.G., 2019. 3-Hydroxyphenylboronic Acid-
626 Based Carbon Dot Sensors for Fructose Sensing. *J. Fluoresc.*, *29*, 265-270.
627 <https://doi.org/10.1007/s10895-018-02336-2>.

628 Crista, D.M.A., El Mragui, A., Algarra, M., Esteves da Silva, J.C.G., Luque, R., Pinto da
629 Silva, L., 2020a. Turning Spent Coffee Grounds into Sustainable Precursors for the Fabrication
630 of Carbon Dots. *Nanomaterials*, *10*, 1209. doi:10.3390/nano10061209.

631 Crista, D.M.A., Esteves da Silva, J.C.G., Pinto da Silva, L., 2020b. Evaluation of Different
632 Bottom-up Routes for the Fabrication of Carbon Dots. *Nanomaterials*, *10*, 1316.
633 <https://doi.org/10.3390/nano10071316>.

634 Deng, Y., Li, J., Qiu, M., Yang, F., Zhang, J., Yuan, C., 2016. Deriving characterization
635 factors on freshwater ecotoxicity of graphene oxide nanomaterial for life cycle impact
636 assessment. *Int J Life Cycle Assess*, *22*, 222–236. <https://doi.org/10.1007/s11367-016-1151-4>.

637 Ding, Y., Tan, W., Zheng, X., Ji, X., Song, P., Bao, L., Zhang, C., Shang, J., Qin, K., Wei,
638 Y., 2020. *Serratia marcescens*-derived fluorescent carbon dots as a platform toward multi-
639 mode bioimaging and detection of p-nitrophenol. *Analyst*, *146*, 683-690.
640 <https://doi.org/10.1039/D0AN01624A>.

641 Eckelman, M.J., Zimmerman, J.B., Anastas, P.T., 2008. Toward Green Nano, E-Factor
642 analysis of several nanomaterial syntheses. *J. Ind. Ecol.*, *12*, 316-328. DOI: 10.1111/j.1530-
643 639 9290.2008.00043.x.

644 Esteves da Silva, J.C.G., Gonçalves, H.M., 2011. Analytical and bioanalytical applications
645 of carbon dots. *TrAC Trends Anal. Chem.*, *30*, 1327-1336.
646 <https://doi.org/10.1016/j.trac.2011.04.009>.

647 Feijoo, S., González-García, S., Moldes-Diz, Y., Vazquez-Vazquez, C., Feijoo, G., Moreira,
648 M.T., 2017. Comparative life cycle assessment of different synthesis routes of magnetic
649 nanoparticles. *J. Clean. Prod.* 143, 528-538. <https://doi.org/10.1016/j.jclepro.2016.12.079>.

650 Fernandes, S., Esteves da Silva, J.C.G., Pinto da Silva, L., 2020. Life Cycle Assessment of the
651 Sustainability of Enhancing the Photodegradation Activity of TiO₂ with Metal-Doping. *Materials*
652 2020, 13(7), 1487. <https://doi.org/10.3390/ma13071487>.

653 He, H., Zheng, X., Liu, S., Zheng, M., Xie, Z., Wang, Y., Yu, M., Shuai, X., 2018.
654 Diketopyrrolopyrrole-based carbon dots for photodynamic therapy. *Nanoscale*, 10, 10991-10998.
655 <https://doi.org/10.1039/C8NR02643B>.

656 Hettiarachchi, S.D., Graham, R.M., Mintz, K.J., Zhou, Y., Vanni, S., Peng, Z., Leblanc, R.M.,
657 2019. Triple conjugated carbon dots as a nano-drug delivery model for glioblastoma brain tumors.
658 *Nanoscale*, 11, 6192-6205. <https://doi.org/10.1039/C8NR08970A>.

659 Hischier, R., Walser, T., 2012. Life cycle assessment of engineered nanomaterials: State of the
660 art and strategies to overcome existing gaps. *Sci. Total Environ.*, 425, 271-282.
661 <https://doi.org/10.1016/j.scitotenv.2012.03.001>.

662 Huijbregts, M.A.J., Steinmann, Z.J.N., Elshout, P.M.F., Stam, G., Verones, F., Vieira, M.,
663 Zipj, M., Hollander, A., van Zelm, R., 2017. ReCiPe2016: a harmonized life cycle impact
664 assessment method at midpoint and endpoint level. *Int. J. Life Cycle Assess.* 22, 138.
665 <https://doi.org/10.1007/s11367-016-1246-y>.

666 Jing, S., Zhao, Y., Sun, R.C., Zhong, L., Peng, X., 2019. Facile and High-Yield Synthesis of
667 Carbon Quantum Dots from Biomass-Derived Carbons At Mild Condition. *ACS Sustainable*
668 *Chem. Eng.*, 7, 7833-7843. DOI: 10.1021/acssuschemeng.9b00027.

669 Kang, Y.F., Li, Y.H., Fang, Y.W., Xu, Y., Wei, X.M., Yin, X.B., 2015. Carbon Quantum Dots
670 for Zebrafish Fluorescence Imaging. *Sci. Rep.*, 5, 11835. DOI: 10.1038/srep11835.

671 Kawakami, M., Suzuki, K., Yokoyama, S., Takenaka, T., 2004. Heat capacity measurement
672 of molten NaNO₃-NaNO₂-KNO₃ by drop calorimetry. *VII International Conference on Molten*
673 *Slags Fluxes and Salts*, The South African Institute of Mining and Metallurgy. 201-208.
674 http://saimm.org.za/Conferences/Slags2004/029_Kawakami.pdf.

675 Knoblauch, R., Geddes, C.D., 2020. Carbon Nanodots in Photodynamic Antimicrobial
676 Therapy: A Review. *Materials*, 13, 4004. <https://doi.org/10.3390/ma13184004>.

677 Kozák, O., Datta, K.K.R., Greplová, M., Ranc, V., Kašlík, J., Zbořil, R., 2013. Surfactant-
678 Derived Amphiphilic Carbon Dots with Tunable Photoluminescence. *J. Phys. Chem. C*, 117,
679 24991-24996. [dx.doi.org/10.1021/jp4040166](https://doi.org/10.1021/jp4040166).

680 Li, L., Lu, C., Li, S., Liu, S., Wang, L., Cai, W., Xu, W., Yang, X., Liu, Y., Zhang, R., 2017.
681 A high-yield and versatile method for the synthesis of carbon dots for bioimaging applications. *J.*
682 *Mater. Chem. B*, 5, 1935. DOI: 10.1039/c6tb03003c.

683 Li, D., Huang, J., Li, R., Chen, P., Chen, D., Cai, M., Liu, H., Feng, Y., Lv, W., Liu, G.,
684 2021. Synthesis of a carbon dots modified g-C₃N₄/SnO₂ Z-scheme photocatalyst with
685 superior photocatalytic activity for PPCPs degradation under visible light irradiation. *J.*
686 *Hazard. Mater.*, 401, 123257. <https://doi.org/10.1016/j.jhazmat.2020.123257>.

687 Lim, S.Y., Shen, W., Gao, Z., 2015. Carbon quantum dots and their applications. *Chem.*
688 *Soc. Rev.*, 44, 362-381. <https://doi.org/10.1039/C4CS00269E>.

689 Liu, Q., Dong, Z., Hao, A., Guo, X., Dong, W., 2021. Synthesis of highly fluorescent
690 carbon dots as a dual-excitation ratiometric fluorescent probe for the fast detection of
691 chlorogenic acid. *Talanta*, 221, 121372. <https://doi.org/10.1016/j.talanta.2020.121372>.

692 Mello, G.P.C., Simões, E.F.C., Crista, D.M.A., Leitão, J.M.M., Pinto da Silva, L., Esteves
693 da Silva, J.C.G., 2019. Glucose Sensing by Fluorescent Nanomaterials. *Crit. Rev. Anal. Chem.*,
694 49, 542-552. <https://doi.org/10.1080/10408347.2019.1565984>.

695 Qiao, G., Chen, G., Wen, Q., Liu, W., Gao, J., Yu, Z., Wang, Q., 2020. Rapid conversion
696 from common precursors to carbon dots in large scale: Spectral controls, optical sensing,
697 cellular imaging and LEDs application. *J. Colloid Interface Sci.*, 580, 88-98.
698 <https://doi.org/10.1016/j.jcis.2020.07.034>.

699 Qiu, Y., Gao, D., Yin, H., Zhang, K., Zeng, J., Wang, L., Xia, L., Zhou, K., Xia, Z., Fu, Q.,
700 2020. Facile, green and energy-efficient preparation of fluorescent carbon dots from processed
701 traditional Chinese medicine and their applications for on-site semi-quantitative visual
702 detection of Cr(VI). *Sens. Actuators B*, 324, 128722.
703 <https://doi.org/10.1016/j.snb.2020.128722>.

704 Pianosi, F., Beven, K., Freer, J., Hall, J.W., Rougier, J., Stephenson, D.B., Wagener, T.,
705 2016. Sensitivity analysis of environmental models: a systematic review with practical
706 workflow. *Environ. Model. Softw* 79, 214-232. <https://doi.org/10.1016/j.envsoft.2016.02.008>.

707 Piccinno, F., Hischer, R., Seeger, S., Som, C., 2016. From laboratory to industrial scale: a
708 scale-up framework for chemical processes in life cycle assessment studies. *J. Clean. Prod.*
709 135, 1085-1097. <http://dx.doi.org/10.1016/j.jclepro.2016.06.164>.

710 Piccinno, F., Hischer, R., Seeger, S., Som, C., 2018. Predicting the environmental impact
711 of a future nanocellulose production at industrial scale: Application of the life cycle
712 assessment scale-up framework. *J. Clean. Prod.* 174, 283-295.
713 <https://doi.org/10.1016/j.jclepro.2017.10.226>.

714 Pourzahedi, L., Eckelman, M.J., 2015. Comparative life cycle assessment of silver
715 nanoparticles synthesis routes. *Environ. Sci.: Nano.*, 2, 361-369.
716 <https://doi.org/10.1039/C5EN00075K>.

717 Pu, Y., Tang, F., Adam, P.M., Laratte, B., Ionescu, R.E., 2016. Fate and Characterization
718 Factors of Nanoparticles in Seventeen Subcontinental Freshwaters: A Case Study on Copper

719 Nanoparticles. *Environ. Sci. Technol.*, *50*, 17, 9370–9379.
720 <https://doi.org/10.1021/acs.est.5b06300>.

721 Ramos, A., Teixeira, C., Rouboa, A., 2018a. Assessment study of an advanced gasification
722 strategy at low temperature for syngas generation. *Int. J. Hydrog. Energy*, *43*, Issue 21, 10155-
723 10166. <https://doi.org/10.1016/j.ijhydene.2018.04.084>.

724 Ramos, A., Teixeira, C., Rouboa, A., 2018b. Environmental Analysis of Waste-to-Energy – A
725 Portuguese Case Study. *Energies* 2018, *11*(3), 548. <https://doi.org/10.3390/en11030548>.

726 Salieri, B., Turner, D.A., Nowack, B., Hischier, R., 2018. Life cycle assessment of
727 manufactured nanomaterials: Where are we? *NanoImpact*, *10*, 108–120.
728 <https://doi.org/10.1016/j.impact.2017.12.003>.

729 Sendão, R.M.S., Crista, D.M.A., Afonso, A.C.P., Martínez de Yuso, M.d.V., Algarra, M.,
730 Esteves da Silva, J.C.G., Pinto da Silva, L., 2019. Insight into the hybrid luminescence showed
731 by carbon dots and molecular fluorophores in solution. *Phys. Chem. Chem. Phys.*, *21*, 20919-
732 20926. <https://doi.org/10.1039/C9CP03730F>.

733 Sendão, R., Martínez de Yuso, M.d.V., Algarra, M., Esteves da Silva, J.C.G., Pinto da Silva,
734 L., 2020. Comparative life cycle assessment of bottom-up synthesis routes for carbon dots derived
735 from citric acid and urea. *J. Clean. Prod.* *254*, 120080.
736 <https://doi.org/10.1016/j.jclepro.2020.120080>.

737 Simões, E.F.C., Pinto da Silva, L., Esteves da Silva, J.C.G., Leitão, J.M.M., 2020.
738 Hypochlorite fluorescence sensing by phenylboronic acid-alizarin adduct based carbon dots.
739 *Talanta*, *208*, 120447. <https://doi.org/10.1016/j.talanta.2019.120447>.

740 Sun, Y.P., Zhou, B., Lin, Y., Wang, W., Fernando, K.A., Pathak, P., Meziani, M.J., Harruff,
741 B.A., Wang, X., Wang, H, Luo, P.G., Yang, H., Kose, M.E., Chen, B., Veca, L.M., Xie, SY.,
742 2006. Quantum-sized carbon dots for bright and colorful photoluminescence. *J. Am. Chem. Soc.*,
743 *128*, 7756-7757. <https://doi.org/10.1021/ja062677d>.

744 Tan, J., Zou, R., Zhang, J., Li, W., Zhang, L., Yue, D., 2016. Large-scale synthesis of N-doped
745 carbon quantum dots and their phosphorescence properties in polyurethane matrix. *Nanoscale*, *8*,
746 4742-4747. <https://doi.org/10.1039/C5NR08516K>.

747 Teah, H.Y., Sato, T., Namiki, K., Asaka, M., Feng, K., Noda, S., 2020. Life Cycle Greenhouse
748 Gas Emissions of Long and Pure Carbon Nanotubes Synthesized via On-Substrate and Fluidized-
749 Bed Chemical Vapor Deposition. *ACS Sustainable Chem. Eng.*, *8*, 1730-1740.
750 <https://dx.doi.org/10.1021/acssuschemeng.9b04542>.

751 Temizel-Sekeryan, S., Hicks, A.L., 2020. Global environmental impacts of silver nanoparticle
752 production methods supported by life cycle assessment. *Resources, Conservation & Recycling*
753 *156*, 1046762, 1-11. <https://doi.org/10.1016/j.resconrec.2019.104676>.

754 Temizel-Sekeryan, S., Wu, F., Hicks, A.L., 2021. Global scale life cycle environmental
755 impacts of single- and multi- walled carbon nanotube synthesis processes. *Int J Life Cycle*
756 *Assess* 26, 656–672. <https://doi.org/10.1007/s11367-020-01862-1>.

757 Tripathi, K.M., Sonker, A.K., Bhati, A., Bhuyan, J., Singh, A., Singh, A., Sarkar, S.,
758 Sonkar, S.K., 2016. Large-scale synthesis of soluble graphitic hollow carbon nanorods with
759 tunable photoluminescence for the selective fluorescent detection of DNA. *New. J. Chem.*, 40,
760 1571-1579. <https://doi.org/10.1039/C5NJ02037A>.

761 Upadhyayula, V., Meyer, D.E., Curran, M.A., Gonzalez, M.A., 2012. Life cycle assessment
762 as a tool to enhance the environmental performance of carbon nanotube products: a review. *J.*
763 *Clean. Prod.*, 26, 37-47. <https://doi.org/10.1016/j.jclepro.2011.12.018>.

764 Vale, N., Silva, S., Duarte, D., Crista, D., Pinto da Silva, L., Esteves da Silva, J.C.G., 2020.
765 Normal breast epithelial MCF-10A cells to evaluate the safety of carbon dots. *RSC Med.*
766 *Chem.* 2021, Advance Article. <https://doi.org/10.1039/D0MD00317D>

767 Van der Hilst, F., Hoefnagels, R., Junginger, M., Londo, M., Shen, L., Wicke, B., 2018.
768 Biomass Provision and Use, Sustainability Aspects. In: Meyers R. (eds) Encyclopedia of
769 Sustainability Science and Technology. Springer, New York, NY.
770 https://doi.org/10.1007/978-1-4939-2493-6_1048-1.

771 Vinsentin, C., Trentin, A.W.S., Braun, A.B., Thomé, A., 2019. Life cycle assessment of
772 environmental and economic impacts of nano-iron synthesis process for application in
773 contaminated site remediation. *J. Clean. Prod.*, 231, 307-319.

774 Wang, R., Gao, Z., Gao, G., Wo, Y., Wang, Y., Shen, G., Cui, D., 2013. Systematic safety
775 evaluation on photoluminescent carbon dots. *Nanoscale Research Letters*, 8:122.
776 <https://doi.org/10.1186/1556-276X-8-122>.

777 Wang, R., Lu, K.Q., Tang, Z.R., Xu, Y.J., 2017a. Recent Progress in carbon quantum dots:
778 Synthesis, properties and applications in photocatalysis. *J. Mater. Chem. A*, 5, 3717-3734.
779 <https://doi.org/10.1039/C6TA08660H>.

780 Wang, Y., Wang, K., Han, Z., Yin, Z., Zhou, C., Du, F., Zhou, S., Chen, P., Xie, Z., 2017b.
781 High color rendering index trichromatic white and red LEDs prepared from silane-
782 functionalized carbon dots. *J. Mater. Chem. C*, 5, 9629-9637.
783 <https://doi.org/10.1039/C7TC02297B>.

784 Wang, C., Hu, T., Chen, Y., Xu, Y., Song, Q., 2019. Polymer-Assisted Self-Assembly of
785 Multicolor Carbon Dots as Solid-State Phosphors for Fabrication of Warm, High-Quality, and
786 Temperature-Responsive White-Light-Emitting Devices. *ACS Appl. Mater. Interfaces*, 11,
787 22332-22338. <https://doi.org/10.1021/acsami.9b04345>.

788 Xie, Y., Cheng, D., Liu, X., Han, A., 2019. Green Hydrothermal Synthesis of N-doped
789 Carbon Dots from Biomass Highland Barley for the Detection of Hg²⁺. *Sensors*, 19, 3169.
790 [doi:10.3390/s19143169](https://doi.org/10.3390/s19143169).

791 Xiong, Y., Schneider, J., Ushakova, E.V., Rogach, A.L., 2018. Influence of molecular
792 fluorophores on the research field of chemically synthesized carbon dots. *Nano Today*, 23, 124-
793 139. <https://doi.org/10.1016/j.nantod.2018.10.010>.

794 Yan, L., Yang, Y., Ma, C.Q., Liu, X., Wang, H., Xu, B., 2016. Synthesis of carbon quantum
795 dots by chemical vapor deposition approach for use in polymer solar cell as the electrode buffer
796 layer. *Carbon*, 109, 598-607. <https://doi.org/10.1016/j.carbon.2016.08.058>.

797 Yang, Y., Cui, J., Zheng, M., Hu, C., Tan, S., Xiao, Y., Yang, Q., Liu, Y., 2012. One-step
798 synthesis of amino-functionalized fluorescent carbon nanoparticles by hydrothermal
799 carbonization of chitosan. *Chem. Commun.*, 48, 380-382. <https://doi.org/10.1039/C1CC15678K>.

800 Yang, G., Wan, X., Su, Y., Zeng, X., Tang, J., 2016. Acidophilic S-doped carbon quantum
801 dots derived from cellulose fibers and their fluorescence sensing performance for metal ions in
802 an extremely strong acid environment. *J. Mater. Chem. A*, 4, 12841-12849.
803 <https://doi.org/10.1039/C6TA05943K>.

804 Zhang, X., Jiang, M., Niu, N., Chen, Z., Li, S., Liu, S., Li, J., 2018. Natural-product-derived
805 carbon dots: from natural products to functional materials. *ChemSusChem*, 11, 11-24. doi:806
806 10.1002/cssc.201701847.

807 Zhang, B., Liu, Y., Ren, M., Li, W., Zhang, X., Vajtal, R., Ajayan, P.M., Tour, J.M., Wang,
808 L., 2019. Sustainable Synthesis of Bright Green Fluorescent Nitrogen-Doped Carbon Quantum
809 Dots from Alkali Lignin. *ChemSusChem*, 12, 4202-4210. DOI:10.1002/cssc.201901693.

810 Zhao, S., Lan, M., Zhu, X., Xue, H., Ng, T.W., Meng, X., Lee, C.S., Wang, P., Zhang, W.,
811 2015. Green Synthesis of Bifunctional Fluorescent Carbon Dots from Garlic for Cellular Imaging
812 and Free Radical Scavenging. *ACS Appl. Mater. Interfaces*, 7, 17054-17060.
813 DOI:10.1021/acsami.5b03228.

814 Zhou, J., Zhou, H., Tang, J., Deng, S., Yan, F., Li, W., Qu, M., 2017. Carbon dots doped with
815 heteroatoms for fluorescent bioimaging: a review. *Microchim. Acta*, 184, 343-368.
816 <https://doi.org/10.1007/s00604-016-2043-9>.

817 Zhou, Y., Liyanage, P.Y., Geleroff, D.L., Peng, Z., Mintz, K.J., Hettiarachchi, S.D., Pandey,
818 R.R., Chusuei, C.C., Blackwelder, P.L., Leblanc, R.M., 2018a. Photoluminescent carbon dots: a
819 mixture of heterogeneous fractions. *ChemPhysChem*, 19, 2589-2597.
820 DOI:10.1002/cphc.201800248.

821 Zhou, D., Wang, Y., Tian, P., Jing, P., Sun, M., Chen, X., Xu, X., Li, D., Mei, S., Liu, X.,
822 Zhang, W., Guo, R., Qu, S., Zhang, H., 2018b. Microwave-assisted heating method toward
823 multicolor quantum dot-based phosphors with much improved luminescence. *ACS Appl. Mater.*
824 *Interfaces*, 10, 27160-27170. DOI: 10.1021/acsami.8b06323.